

Role of Solvent Dynamics in Stabilizing the Transition State of RNA Hydrolysis by Hairpin Ribozyme

Hwangseo Park^{*,†} and Sangyoub Lee^{*,‡}

Department of Bioscience and Biotechnology, Sejong University, 98 Kunja-Dong, Kwangjin-Ku, Seoul 143-747, Korea, and Department of Chemistry, Seoul National University, Seoul 151-747, Korea

Received December 1, 2005

Abstract: Structural and mechanistic studies of the hairpin ribozyme have been actively pursued over the last two decades to understand its catalytic strategy for RNA hydrolysis. Based on molecular dynamics simulations with the newly developed force field parameters for a vanadium–oxygen complex, we investigate the dynamic properties of the hairpin ribozyme in complex with a transition state analogue for the phosphodiester cleavage. The results indicate that the three nucleobases of the hairpin ribozyme (G8, A9, and A38) stabilize the negatively charged oxygen atoms in the transition state through the formation of five hydrogen bonds, which is consistent with the X-ray crystallographic data. In addition to the three catalytic nucleobases, several solvent molecules are also found to contribute to the catalytic action of the hairpin ribozyme by hydrogen bond stabilization of the negatively charged oxygens as well as by optimally positioning the catalytic nucleobases in the active site.

Introduction

The hairpin ribozyme catalyzes the reversible and sequence-specific cleavage of phosphodiester backbone of an RNA substrate.¹ This catalytic transesterification reaction is facilitated by the intramolecular attack of the neighboring 2'-hydroxy moiety on the phosphorus atom, leading to the formation of a cyclic phosphorane intermediate or transition state that precedes 2',3'-cyclic phosphate and 5'-hydroxyl termini (Figure 1). In the past two decades, numerous studies with a variety of model systems have been carried out to clarify the underlying chemical principles of the catalytic cleavage of RNA.² It was suggested that although divalent metal ions, Mg²⁺ in particular, stabilize the structure of the hairpin ribozyme in a functionally active form, they are known to be nonessential in the catalytic mechanism, contributing at most a 10–20-fold to rate enhancement.^{3–5} This indicates that the major role in the catalytic mechanism

of the hairpin ribozyme should be played by the nucleobases themselves, possibly involving the general acid–base mechanism⁶ to stabilize the unfavorable charges developing in the transition state.

A few years ago, high-resolution X-ray crystal structures of the hairpin ribozyme were reported in complex with a noncleavable substrate analogue or a transition state mimic including a pentavalent vanadium ion.⁷ These structures suggested a model for ribozyme catalysis in which the nucleobases of G8, A9, and A38 serve as the electrophilic catalysts that stabilize the transition state by donating multiple hydrogen bonds. The crystal structures also revealed that A38 acts as a hydrogen bond donor to the leaving O5' atom in its protonated form at N1 position. However, recent kinetic studies disproved the critical roles of the nucleobases, especially with regards to G8 in general acid-general base catalysis of the hairpin ribozyme.^{8,9} Although the involvement of water molecule(s) in the catalytic mechanism of ribozymes has been proposed,^{10,11} no ordered water molecule was detected near the active site of hairpin ribozyme in the X-ray crystal structures. Therefore, the precise role of water molecule(s) in the catalytic mechanism of the hairpin ribozyme still remains unclear.

* Correspondence may be addressed to either author. Phone: +82-2-3408-3766. Fax: +82-2-3408-3334. E-mail: hspark@sejong.ac.kr (H.P.); sangyoub@snu.ac.kr (S.L.).

[†] Sejong University.

[‡] Seoul National University.

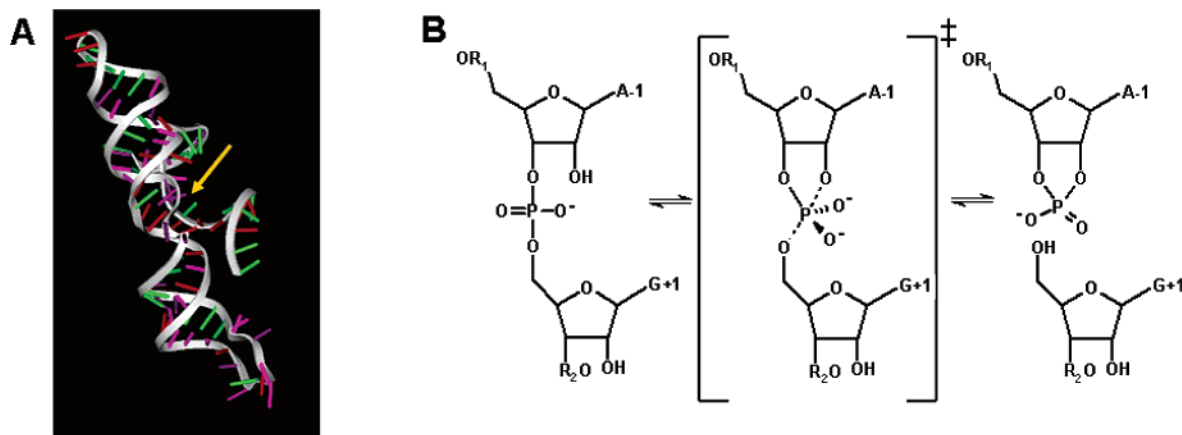


Figure 1. (A) Crystal structure of the hairpin ribozyme. Indicated by a yellow arrow is the catalytic site in which a substrate RNA is hydrolyzed. (B) Schematic of the reversible transesterification reaction of a substrate RNA catalyzed by the hairpin ribozyme.

In this paper, we report the dynamic properties of the hairpin ribozyme in complex with the vanadate transition state analogue based on molecular dynamics (MD) simulation in aqueous solution. We focus our interest on clarifying the roles of solvent molecules in maintaining the structure of the hairpin ribozyme and in stabilizing the transition state. Also presented are the potential parameters for the vanadium–oxygen complex mimicking the transition state of the phosphodiester cleavage, which are unavailable in the current force field database. The detailed structural and dynamic features found in this MD study are expected to provide new insight into the catalytic mechanism of the hairpin ribozyme.

Computational Methods

A. Force Field Design for the Vanadium–Oxygen Complex. To obtain the missing force field parameters, we used a simplified structural model for the hairpin ribozyme in complex with the transition state mimic. This model structure includes the two riboses of (A – 1) and (G + 1) residues and the bridging vanadium ion whose coordinates were extracted from the original X-ray structure. The two nucleobases were omitted for simplicity. We adopted the bonded approach proposed by Hoops et al.¹² to introduce explicit bonds between the central pentavalent vanadium ion and its oxygen ligands. In the derivation of the missing force field parameters, we followed the procedure suggested by Fox and Kollman¹³ to be consistent with the standard AMBER force field.¹⁴ The equilibrium bond lengths and bond angles involving the pentavalent vanadium ion were computed using the optimized structure of the vanadium–oxygen complex mimicking the transition state of the phosphodiester cleavage. For the force constant parameters associated with the vanadium ion, we used those for the sugar–phosphate backbone of RNA or DNA that are available in the force field database. The Lennard-Jones parameters of the backbone phosphorus atom were used for the vanadium ion. Geometry optimization of the vanadium–oxygen complex was performed at the B3LYP/6-31G* level of theory with the Gaussian98 program. Using the energy-minimized structure, atomic partial charges for the transition state mimic were also calculated at the RHF/6-31G* level of theory through the RESP method¹⁵ to be consistent with the standard AMBER force field. We computed the potential parameters

for the protonated adenine at N1 position by following the same procedure as for the vanadium–oxygen complex, which involves geometry optimization and charge fitting with the RESP method.

B. MD Simulations. As a starting structure of MD simulation with the AMBER7 program,¹⁶ we used the X-ray crystal structure of the hairpin ribozyme in complex with a vanadate transition state analogue (PDB entry: 1M5O). In addition to the 37 Ca²⁺ ions in the original X-ray structure, 29 Na⁺ ions were added to neutralize the negative charges of the system. The all-atom model for the complex was then immersed in a rectangular box containing 11 891 TIP3P¹⁷ water molecules. After 1000 cycles of energy minimization (500 steps for solvent molecules only followed by 500 steps for the entire system with no restraints) to remove bad steric contacts, we equilibrated the ribozyme-transition state mimic complex beginning with 20 ps equilibration dynamics of the solvent molecules at 300 K. The next step involved equilibration of the solute with a fixed configuration of the solvent molecules for 10 ps at 10, 50, 100, 150, 200, 250, and 300 K. These partial equilibrations were used to ensure the stability of the entire system although the full equilibration had been more conventional.¹⁸ Then, the equilibration dynamics of the entire system was performed at 300 K for 100 ps. Following the equilibration procedure, 1.8 ns MD simulations were carried out with a periodic boundary condition in the NPT ensemble at 300 K using Berendsen temperature coupling¹⁹ and constant pressure (1 atm) with isotropic molecule-based scaling. The SHAKE algorithm,²⁰ with a tolerance of 10^{–6}, was applied to fix all bond lengths involving hydrogen atom. We used a time step of 1.0 fs and a nonbond-interaction cutoff radius of 12 Å; the trajectory was sampled every 0.2 ps (200 step intervals) for analysis.

Results and Discussion

To extend the AMBER force field for modeling the vanadium–oxygen complex that mimics the transition state of the phosphodiester cleavage, we used the standard procedure that starts with the geometry optimization of the complex at the B3LYP/6-31G* level of theory. Figure 2 displays the structure of a local energy minimum whose input structure was extracted from the X-ray crystal structure of the hairpin ribozyme in complex with the vanadate transition

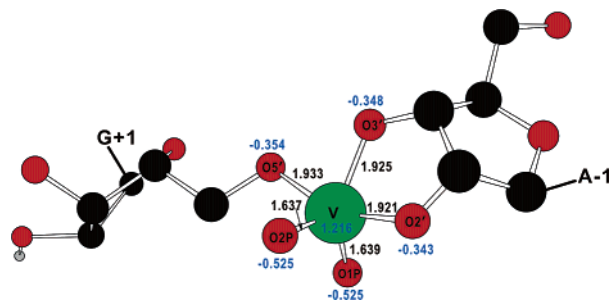


Figure 2. Optimized structure of the vanadium–oxygen complex mimicking the transition state of the phosphodiester cleavage. The calculated RESP atomic charges and the V–O coordination distances are given in e and Å, respectively. All hydrogen atoms bonded to carbon atoms are omitted for simplicity.

state mimic.⁸ Also presented are the calculated RESP atomic charges and the coordination distances between the vanadium ion and its oxygen ligands. Consistent with the crystal structure, the five oxygen ligands are coordinated to the central vanadium ion to form a distorted trigonal bipyramidal geometry. The interatomic distances associated with the V–O coordination compare reasonably well with those in the crystal structure with a difference of 0.028 Å on average.

In Figure 2, it is noted that the RESP atomic charge of the pentavalent vanadium ion decreases from +5.000 e in the free state to +1.216 e in the coordination complex. On the other hand, the atomic charges of oxygen ligands become less negative by 0.145–0.271 e when compared to those in the absence of the vanadium ion. These changes reflect the redistribution of charges between the vanadium ion and its oxygen ligands upon the formation of the complex. We used these newly obtained atomic charges in the subsequent MD simulation of the hairpin ribozyme in complex with the transition state mimic because it is well-attested that the M^{n+} model for a metal ion is inadequate for maintaining the actual coordination geometry of a transition metal complex contained in biomolecules.²¹

We checked the reliability of current MD simulation by examining whether the structure of the hairpin ribozyme was maintained stable under the simulation condition described in the previous section. For this purpose, we calculated the root-mean-square-deviations from starting structure ($\text{RMSD}_{\text{init}}$) for all backbone heavy atoms of the hairpin ribozyme and for all heavy atoms of the transition state mimic as a function of simulation time, which are compared in Figure 3. The computed $\text{RMSD}_{\text{init}}$ values for the hairpin ribozyme remain within 2.5 Å, indicating that the conformation of hairpin ribozyme is maintained stable during the entire course of simulation. The $\text{RMSD}_{\text{init}}$ values of the transition state mimic fall into 1.5 Å and remain lower than those of the backbone atoms of the hairpin ribozyme. Judging from this difference in dynamic behavior, the movement of the transition state mimic around the active site seems to be insignificant when compared to the conformational change of the hairpin ribozyme.

Shown in Figure 4 is the representative MD trajectory snapshot of the hairpin ribozyme in complex with the transition state mimic. As in the crystal structure reported by Rupert et al.,⁸ the nucleophilic 2'OH at the cleavage site

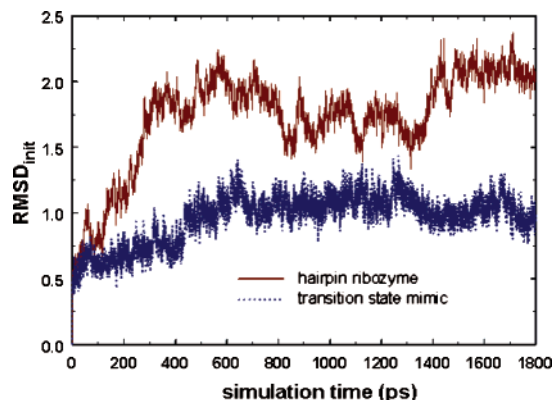


Figure 3. Comparative view of the time evolutions of the root-mean-square deviations for backbone heavy atoms of the hairpin ribozyme (red) and all heavy atoms of the transition state mimic (blue).

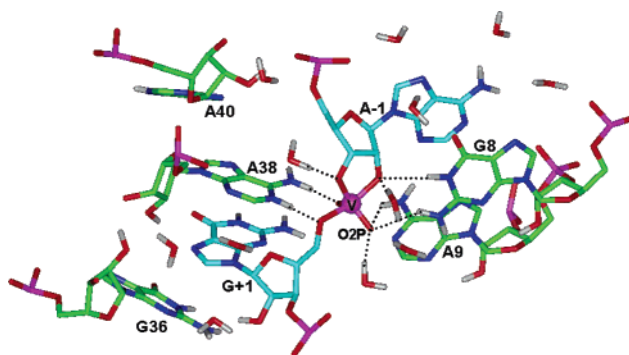


Figure 4. Representative MD trajectory snapshot of the hairpin ribozyme in complex with the vanadate transition state mimic including the water molecules found near the active site. Carbon atoms of the hairpin ribozyme and the transition state mimic are indicated in green and cyan, respectively. Each dotted line indicates a hydrogen bond.

(A – 1) of the transition state mimic, vanadium ion, and the 5' oxygen of the leaving group (G + 1) reside in nearly optimal positions for an in-line $\text{S}_{\text{N}}2$ -type reaction mechanism. It is also consistent with the X-ray structure that the three nucleobases of the hairpin ribozyme (G8, A9, and A38) donate five hydrogen bonds to stabilize the oxygen atoms coordinated to the vanadium ion. In this solution-phase structure, O2' and O3' atoms of the (A – 1) residue and O2P atoms of the (G + 1) residue are further stabilized by forming three hydrogen bonds with the water molecules that diffuse into the active site of the hairpin ribozyme from bulk solvent. This is a structural feature inconsistent with the X-ray crystal structure in which no ordered water molecule was found within the distance of 10 Å from the vanadium ion although the transition state mimic occupies a small portion of the active site volume and leaves sufficient space for additional molecules to get into the active site. Related with such a discrepancy, it can be argued that the access of water molecules to the active site may depend on the crystallization procedure. The presence of a hydrogen bond between the deprotonated O2' atom of the (A – 1) residue and a water molecule supports the possibility that the role of proton acceptor for the nucleophilic oxygen of an RNA

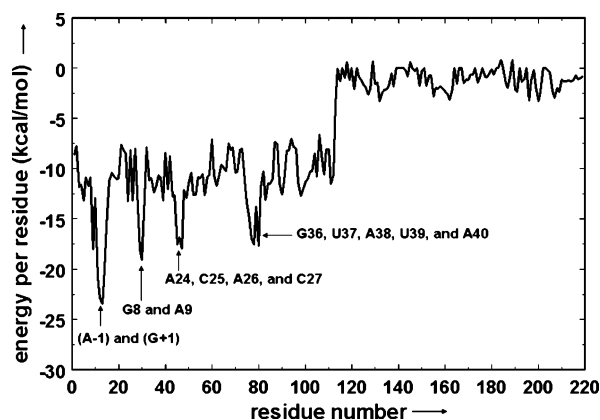


Figure 5. Interaction energy per residue for the average structure of the hairpin ribozyme in complex with the transition state mimic. Residues 1–21, 22–113, and 114–220 correspond to the transition state mimic, the hairpin ribozyme, and the solvent molecules found within 5 Å around the transition state mimic, respectively.

substrate should be played by water in the catalytic mechanism of the hairpin ribozyme.

To provide further evidence for strong interactions between the transition state mimic and the catalytic nucleobases and solvent molecules, we calculate the interaction energy per residue for the average structure of the complex. As indicated in Figure 5, the most significant contributions to the stabilization of the complex seem to come from the interaction between (A – 1) and (G + 1) residues of the transition state mimic and the catalytic nucleobases including G8, A9, C25, A24, C25, A26, C27, G36, U37, A38, U39, and A40. However, no solvent molecule is found that can stabilize the transition state mimic as comparable to the catalytic nucleobases. Possible reasons for this may include the small size of water molecule and the exchange of the water molecules donating hydrogen bonds to the transition state mimic.

To estimate dynamic stabilities of the hydrogen bonds relevant to the stabilization of the transition state mimic, we have calculated time evolutions of the associated interatomic

distances, which are plotted in Figure 6. We note that the hydrogen bondings of the catalytic nucleobases to the transition state mimic are maintained stable during the entire course of simulation with 95% of residence time on average. Similarly, all three hydrogen bonds established between water molecules and the transition state mimic are maintained for more than 80% of simulation time if the distance limit for the O···H hydrogen bond is assumed to be 2.2 Å as suggested by Jeffrey.²² In contrast to the obvious dynamic stabilities of the hydrogen bondings to the transition state mimic by the three catalytic nucleobases, however, we find that there are exchanges of the water molecules that act as a hydrogen bond donor with respect to the transition state mimic. This indicates the involvement of complex solvent dynamics in an optimal stabilization of the transition state by the hairpin ribozyme. It is noteworthy that as shown in Figure 7, the three O···H–O hydrogen bond angles between water molecules and the transition state mimic are also maintained stable during the entire course of simulation. This implies that a complex solvent dynamics would have an insignificant effect on the strengths of the three hydrogen bonds. Thus, the structural and dynamical features found in this MD study support the hypothesis that the hairpin ribozyme has evolved to maximize its hydrogen bonding interactions with the trigonal bipyramidal transition state.

Conclusions

We have developed the force field parameters appropriate for modeling the vanadate transition state mimic for the phosphodiester cleavage by the hairpin ribozyme. The hairpin ribozyme in complex with the transition state mimic shows a dynamic stability in aqueous solution, maintaining a square bipyramidal coordination geometry at the reaction center including the nucleophilic 2'OH at the cleavage site (A – 1), vanadium ion, and the 5' oxygen of the leaving group (G + 1). This supports the S_N2-type reaction mechanism of the hairpin ribozyme. As in the crystal structure, the three nucleobases of the hairpin ribozyme (G8, A9, and A38) stabilize the negatively charged oxygen atoms in the transition state mimic through the formation of five hydrogen

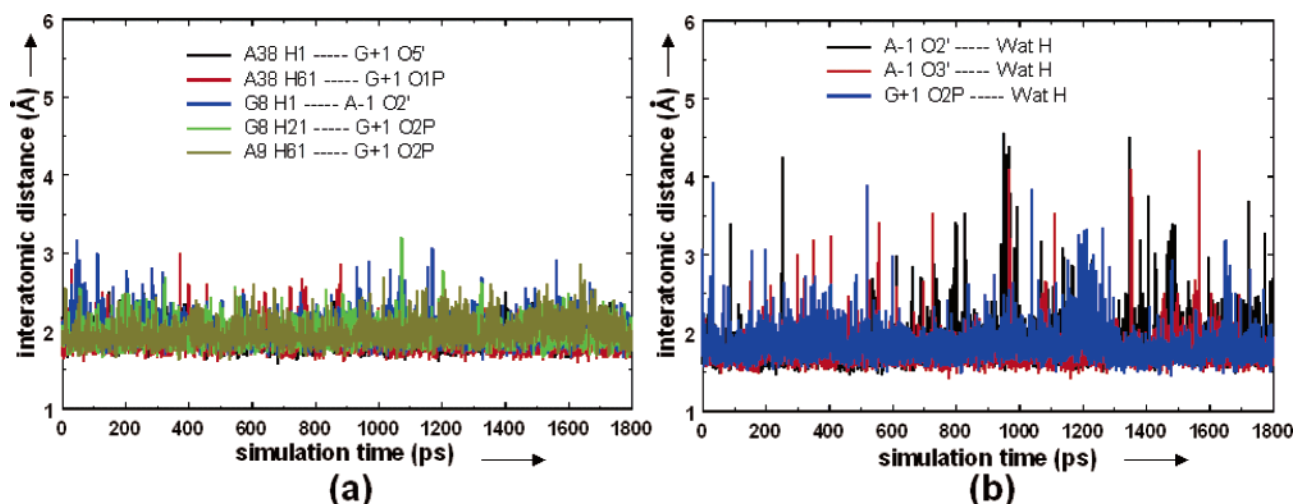


Figure 6. Time evolutions of the interatomic distances associated with hydrogen-bond interactions (a) between catalytic nucleobases of hairpin ribozyme and vanadate transition state mimic and (b) between solvent molecules and the transition state mimic.

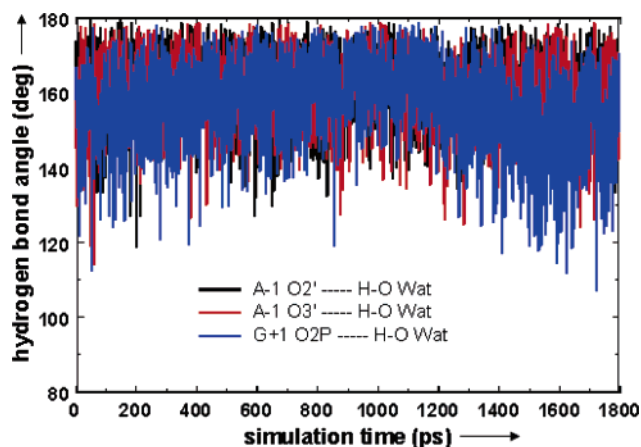


Figure 7. Time evolutions of the O...H-O angles associated with the hydrogen bonds between the transition state mimic and solvent molecules.

bonds. Several solvent molecules are also found to contribute to the catalytic action of the hairpin ribozyme by hydrogen bond stabilization of the negatively charged oxygens and by optimally positioning the catalytic nucleobases in the active site. The presence of a hydrogen bond between the deprotonated O2' atom at the (A - 1) site and a solvent molecule supports the possibility that the nucleophilic oxygen of an RNA substrate would be deprotonated by water in bulk solvent during the catalytic action of the hairpin ribozyme.

Acknowledgment. This work was supported by Grant No. R01-2004-000-10354-0 from the Basic Research Program of the Korea Science & Engineering Foundation. The authors would also like to acknowledge the support from KISTI (Korea Institute of Science and Technology Information) under "The Seventh Strategic Supercomputing Support Program" with Dr. Sang Min Lee as the technical supporter. The use of the computing system of the Supercomputing Center is greatly appreciated.

Note Added after ASAP Publication. This article was released ASAP on March 14, 2006, with the incorrect Received Date. The correct version was posted on April 13, 2006.

Supporting Information Available: Force field parameters of the vanadium-oxygen complex used to represent the transition state mimic. This material is available free of charge via the Internet at <http://pubs.acs.org>.

References

- (1) Fedor, M. J. Structure and function of the hairpin ribozyme. *J. Mol. Biol.* **2000**, *297*, 269–291.
- (2) DeRose, V. J. Two Decades of RNA Catalysis. *Chem. Biol.* **2002**, *9*, 961–969.
- (3) Curtis, E. A.; Bartel, D. P. The hammerhead cleavage reaction in monovalent cations. *RNA* **2001**, *7*, 546–552.
- (4) O'Rear, J. L.; Wang, S.; Feig, A. L.; Beigelman, L.; Uhlenbeck, O. C.; Herschlag, D. Comparison of the hammerhead cleavage reactions stimulated by monovalent and divalent cations. *RNA* **2001**, *7*, 537–545.
- (5) Nakano, S.; Proctor, D. J.; Bevilacqua, P. C. Mechanistic characterization of the HDV genomic ribozyme: assessing the catalytic and structural contributions of divalent metal ions within a multichannel reaction mechanism. *Biochemistry* **2001**, *40*, 12022–12038.
- (6) Bevilacqua, P. C. Mechanistic considerations for general acid-base catalysis by RNA: revisiting the mechanism of the hairpin ribozyme. *Biochemistry* **2003**, *42*, 2259–2265.
- (7) Rupert, P. B.; Massey, A. P.; Sigurdsson, S. Th.; Ferre-D'Amare, A. R. Transition state stabilization by a catalytic RNA. *Science* **2002**, *298*, 1421–1424.
- (8) Kuzmin, Y. I.; Da Costa, C. P.; Fedor, M. J. Role of an active site guanine in hairpin ribozyme catalysis probed by exogenous nucleobase rescue. *J. Mol. Biol.* **2004**, *340*, 233–251.
- (9) Kuzmin, Y. I.; Da Costa, C. P.; Cottrell, J. W.; Fedor, M. J. Role of an active site adenine in hairpin ribozyme catalysis. *J. Mol. Biol.* **2005**, *349*, 989–1010.
- (10) Nakano, S.; Chadalavada, D. M.; Bevilacqua, P. C. General acid-base catalysis in the mechanism of a hepatitis delta virus ribozyme. *Science* **2000**, *287*, 1493–1497.
- (11) Shih, I.; Been, M. D. Catalytic strategies of the hepatitis delta virus ribozymes. *Annu. Rev. Biochem.* **2002**, *71*, 887–917.
- (12) Hoops, S. C.; Anderson, K. W.; Merz, K. M., Jr. Force field design for metalloproteins. *J. Am. Chem. Soc.* **1991**, *113*, 8262–8270.
- (13) Fox, T.; Kollman, P. A. Application of the RESP methodology in the parameterization of organic solvents. *J. Phys. Chem. B* **1998**, *102*, 8070–8079.
- (14) Cornell, W. D.; Cieplak, P.; Bayly, C. I.; Gould, I. R.; Merz, K. M., Jr.; Ferguson, D. M.; Spellmeyer, D. C.; Fox, T.; Caldwell, J. W.; Kollman, P. A. A second generation force field for the simulation of proteins, nucleic acids, and organic molecules. *J. Am. Chem. Soc.* **1995**, *117*, 5179–5197.
- (15) Bayly, C. A.; Cieplak, P.; Cornell, W. D.; Kollman, P. A. A well behaved electrostatic potential based method using charge restraints for deriving atomic charges: the RESP model. *J. Phys. Chem.* **1993**, *97*, 10269–10280.
- (16) Case, D. A.; Cheatham, T. E., III; Darden, T.; Gohlke, H.; Luo, R.; Merz, K. M., Jr.; Onufriev, A.; Simmerling, C.; Wang, B.; Woods, R. J. The Amber biomolecular simulation programs. *J. Comput. Chem.* **2005**, *26*, 1668–1688.
- (17) Jorgensen, W. L.; Chandrasekhar, J.; Madura, J. D.; Impey, R. W.; Klein, M. L. Comparison of simple potential functions for simulating liquid water. *J. Chem. Phys.* **1983**, *79*, 926–935.
- (18) Beveridge, D. L.; Dixit, S. B.; Barreiro, G.; Thayer, K. M. Molecular dynamics simulations of DNA curvature and flexibility. *Biopolymers* **2004**, *73*, 380–403.
- (19) Berendsen, H. C.; Postma, J. P. M.; van Gunsteren, W. F.; DiNola, A.; Haak, J. R. Molecular dynamics with coupling to an external bath. *J. Chem. Phys.* **1984**, *81*, 3684–3690.
- (20) Ryckaert, J. P.; Cicciotti, G.; Berendsen, H. C. Numerical integration of the cartesian equations of motion of a system with constraints: molecular dynamics of *n*-alkanes. *J. Comput. Phys.* **1977**, *23*, 327–341.
- (21) Stote, R. H.; Karplus, M. Zinc binding in proteins and solution: a simple but accurate nonbonded representation. *Proteins* **1995**, *23*, 12–31.
- (22) Jeffrey, G. A. *An Introduction to Hydrogen Bonding*; Oxford University Press: Oxford, 1997.